SITC 2023 Abstract#1301

High-throughput analysis of immune biomarkers from brightfield whole tumor images using Indica HALO®

Jeff Lock · Nam Tran · James Hargrove · Ben Ovadia · Harry Nunns · Qingyan Au · Arezoo Hanifi

NeoGenomics Laboratories, Aliso Viejo, CA

Introduction

A comprehensive understanding of the tumor microenvironment (TME) empowers researchers/scientists in the field of immuno-oncology to develop clinical diagnostic tests and targeted therapeutic interventions. Historically, such research relied on the manual examination of pathological tissue biopsy sections by medical pathologists. By combining whole-slide imaging with quantitative tissue analysis using machine learning, digital pathology offers the potential to transform this tedious, manual-practice into a scalable/high-throughput, easy to use process and enable deeper insight into TME oncology studies. A major challenge to realizing this potential is the development of image analysis (IA) algorithms capable of faithfully replicating manual interpretation of the specimen. Here, we present a workflow for the development and validation of IA algorithms for tissue classification and the detection of molecular biomarkers from digitized whole-slide image/specimens of tumor tissues acquired by brightfield microscopy. The CD8 detection algorithm presented here has been validated for clinical sample testing.

Methods

Digitized whole-slide images of NSCLC tissues stained for CD8 and corresponding serial H&E images were used in this study. H&E and CD8 IHC images were sent to pathologist for tissue classification and manual scoring, respectively. The pathologist determined positive cells counts from IHC images within randomly chosen regions of interest (ROIs) encompassing both tumor and stromal regions. Pathologist scored images were then divided into training and validation sets for algorithm development. IA algorithms were developed in the HALO® platform which has been previously GxP validated by NeoGenomics. Tissue segmentation and biomarker detection algorithms were developed on the training set to classify tumor and stromal regions and identify CD8 positive cells. Algorithm performance was visually inspected by a pathologist and CD8 detection evaluated for concordance with pathologist manual scores. Once the algorithms were established against the training set, they were validated on the validation image set. For all images, analysis results provided counts, percentages and densities for all tumor and stromal regions in the tissue specimen.

Results

For tissue classification of H&E images, similarity between pathologist-determined and algorithm-generated annotations were assessed by the mean square error between binary image masks of the annotations and expressed as a percent difference between images. Results showed, on average, a less than 10% difference between algorithm-generated and pathologist-determined annotations of tumor and stromal regions.

For biomarker detection in IHC images, the concordance of pathologist manual scores and Halo algorithmic results were evaluated using the Pearson correlation coefficient. The results showed concordance above 85% for percent CD8 positive cells in the validation dataset.

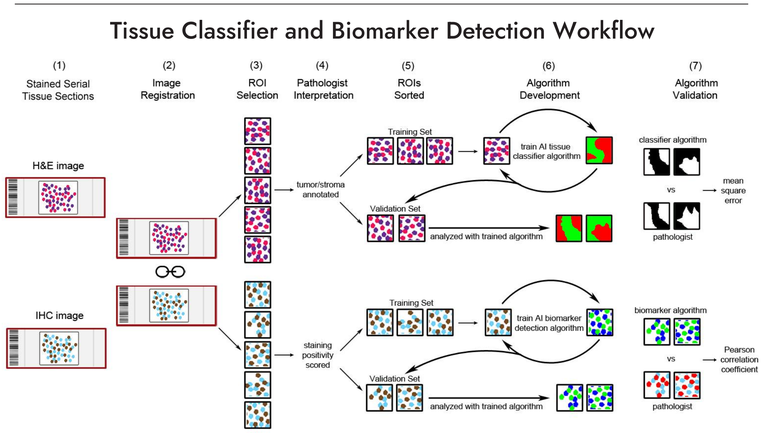

Figure 1. Image analysis workflow the development and validation of tissue classifier and biomarker detection algorithms in Indica Halo. (1) Serial tissue sections were stained by H&E and labeled for CD8 by IHC. (2) Images were linked by image registration in Halo. (3) ROIs were randomly selected from H&E and IHC images and (4) sent to pathology for annotation of tumor and stromal regions and for scoring of biomarker positivity, respectively. (5) ROIs were randomly sorted into mutually exclusive training and validation image sets and (6) AI algorithms were trained on the training set images for the classification of tumor and stromal regions from H&E images and the detection of CD8 from IHC images. The validation image set was analyzed by the trained algorithms. (7) Validation of the tissue classifier algorithm was performed by mean square error analysis between binarized algorithm-generated and pathologist-determined annotations. Validation of the biomarker detection algorithm was performed by concordance between algorithms counts and pathologist counts of CD8 positive cells by Pearson correlation coefficient analysis.

Tissue Classification

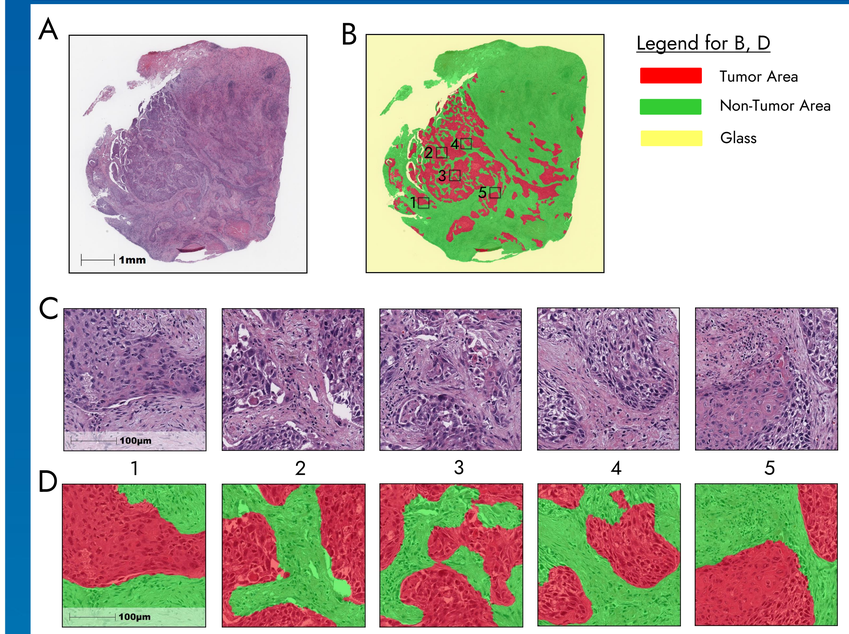

Figure 2: **Classification of whole-slide NSCLC H&E images into tumor and non-tumor regions.** A) Representative whole slide H&E image. B) Overlay of the trained AI tissue classifier depicting tumor in red, nontumor in green, and slide glass in yellow. C) Magnified H&E tissue regions corresponding to the labeled ROIs in panel B and D) matched images displaying the tissue classifier overlays.

Biomarker Detection

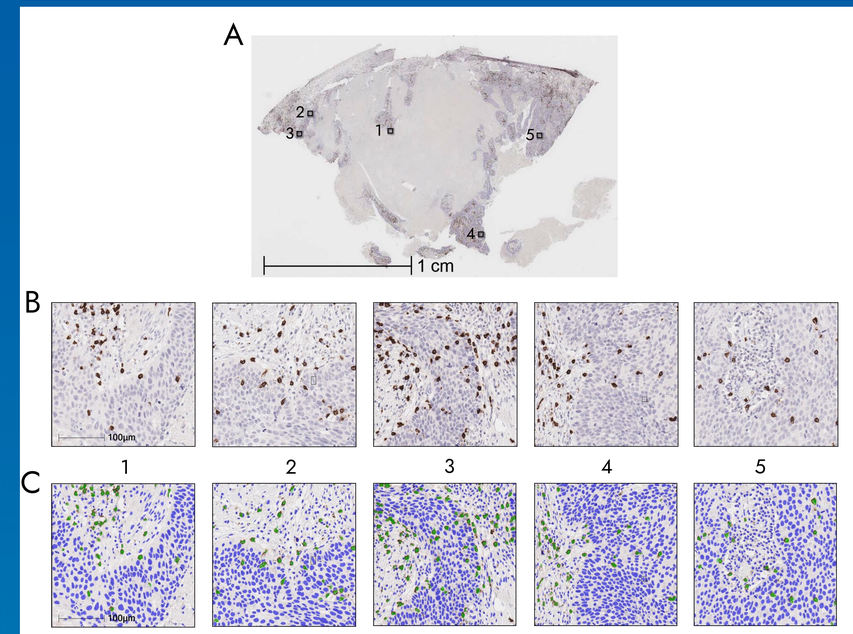

Figure 5: Biomarker detection in whole-slide IHC images stained for CD8. A) Representative whole slide IHC image. B) Magnified IHC tissue regions (100,000 µm²) corresponding to the labeled ROIs in panel A and C) matched images displaying overlays of the AI-trained detection algorithm depicting CD8 positive cells in green and CD8 negative cells in blue.

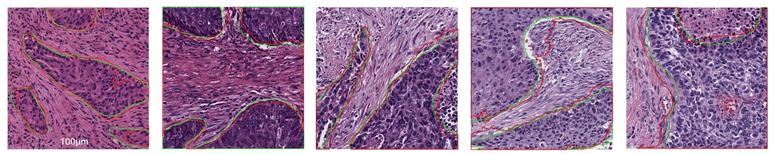

Figure 3: AI-generated vs. hand-drawn tumor annotations. H&E images show red and green lines depicting AI-generated and hand-drawn annotations, respectively. Each image is a 100,000 µm² region from a different image/specimen.

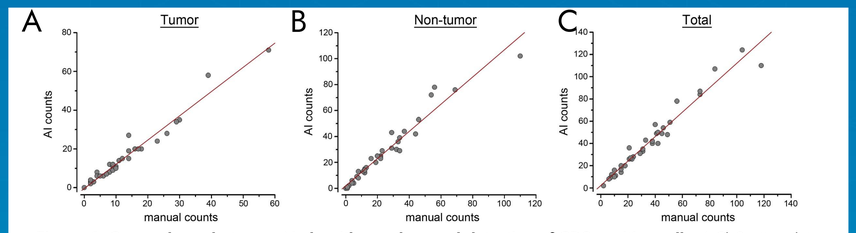

Figure 6: Concordance between AI algorithm and manual detection of CD8 positive cells. A-C) Scatter plots show the number of CD8 positive cells detected by the algorithm compared to visual inspection in tumor regions (A), non-tumor regions (B) or both (C); n = 36 ROIs. Red lines depict the regression fit with a slope of 1.2 (A), 1.0 (B), and 1.1 (C). Pearson correlation coefficient between AI and manual counts was 0.98 (A), 0.97 (B), and 0.97 (C).

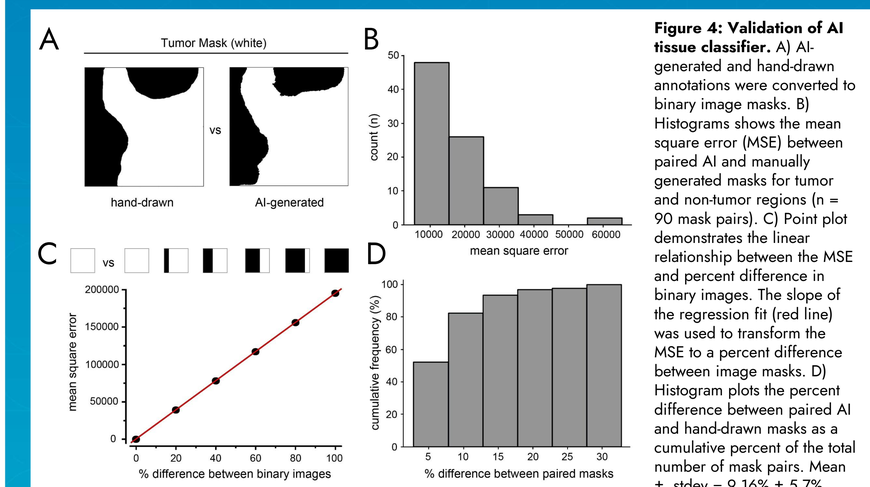

Figure 4: Validation of AI tissue classifier. A) AI-generated and hand-drawn annotations were converted to binary image masks. B) Histograms shows the mean square error (MSE) between paired AI and manually generated masks for tumor and non-tumor regions (n = 90 mask pairs). C) Point plot demonstrates the linear relationship between the MSE and percent difference in binary images. The slope of the regression fit (red line) was used to transform the MSE to a percent difference between image masks. D) Histogram plots the percent difference between paired AI and hand-drawn masks as a cumulative percent of the total number of mask pairs. Mean ± stdev = 9.16% ± 5.7%.

Summary

- The trained Halo AI tissue classifier generates tumor and stromal annotations with a high degree of similarity to hand-drawn annotations by a pathologist, as demonstrated by mean square error analysis – a nonbiased, quantitative method for evaluating tissue classifier performance on a pixel-by-pixel basis
- The trained Halo AI CD8 biomarker detection algorithm, achieved a high concordance to the manual detection of CD8 positive cells as determined by Pearson correlation coefficient
- Pathologist-guided image analysis development yields tissue classifier and biomarker-specific algorithms capable of segmenting and analyzing tissue image/specimens with a high-degree of accuracy, providing a robust, scalable solution for discovery-based research efforts and clinical drug trials

NEO GENOMICS